Soils and Foundations 2014;54(3):250–268

The Japanese Geotechnical Society

Soils and Foundations

www.sciencedirect.com
journal homepage: www.elsevier.com/locate/sandf

Response of framed buildings to excavation-induced movements

Kok Hun Goh[a,*], Robert James Mair[b,1]

[a]Land Transport Authority, No. 1, Hampshire Road, Singapore 219428, Singapore
[b]Engineering Department,. University of Cambridge, Trumpington Street, Cambridge, CB2 1PZ, UK

Received 11 July 2012; received in revised form 23 May 2013; accepted 18 June 2013
Available online 13 May 2014

Abstract

This paper presents a study of the influence of frame action on the response of buildings to deformations induced by deep excavations in soft clay. Using the finite element method, a building was modelled as a framed structure adjacent to a multi-propped excavation, firstly as a frame with continuous footings and then as a frame with individual footings. The geometry, location, and structural elements forming the frame models were varied to investigate the response of various frames. Using a structural analysis, parameters representing the stiffness of the frames in reducing deflection ratios and horizontal strains were derived. The influence of the frame action on the building stiffness can be quantified using the results from the finite element models. This makes it possible to estimate building modification factors from the relevant design charts so that induced deflection ratios and horizontal strains, caused by adjacent excavation and tunnelling activities, can be calculated. The approach gives a more realistic estimate of the tensile strains for assessing the potential damage caused to buildings.

Keywords: Building response; Excavations; Frame action

1. Introduction

1.1. Background

Buildings vary so much in structural concept and detail that it is difficult to lay down general guidelines for the influence of settlements on building serviceability and performance. Nevertheless, from full scale model tests conducted by the Building Research Station, in which masonry walls and infill frames were forced to deflect like simple beams, Burland and Wroth (1974) noted that the onset of visible cracking was related to the induced tensile strains. They proposed using the deflection of a centrally loaded simple beam as an idealised representation of the deflection of actual buildings, and used Timoshenko's beam theory to derive equations relating the deflection ratio to tensile strains using the beam's geometric and stiffness properties. These were supported using observations of the damage to a number of buildings together with the observations from full-scale model tests (Burland et al., 1977). Since then, these equations have been re-written and are now the basis for estimating the potential building damage caused by tunnelling- and excavation-induced deformations.

The procedure for building damage assessment, outlined by Mair et al. (1996), was based on deflection ratios and horizontal strains in the *greenfield* condition. This ignores the inherent stiffness in buildings and is conservative. To include

*Corresponding author. Tel.: +65 6396 1494.
E-mail addresses: kok_hun_goh@lta.gov.sg (K.H. Goh), rjm50@cam.ac.uk (R.J. Mair).
[1]Tel.: +44 1223 332631.
Peer review under responsibility of The Japanese Geotechnical Society.

Production and hosting by Elsevier

http://dx.doi.org/10.1016/j.sandf.2014.04.002
0038-0806/

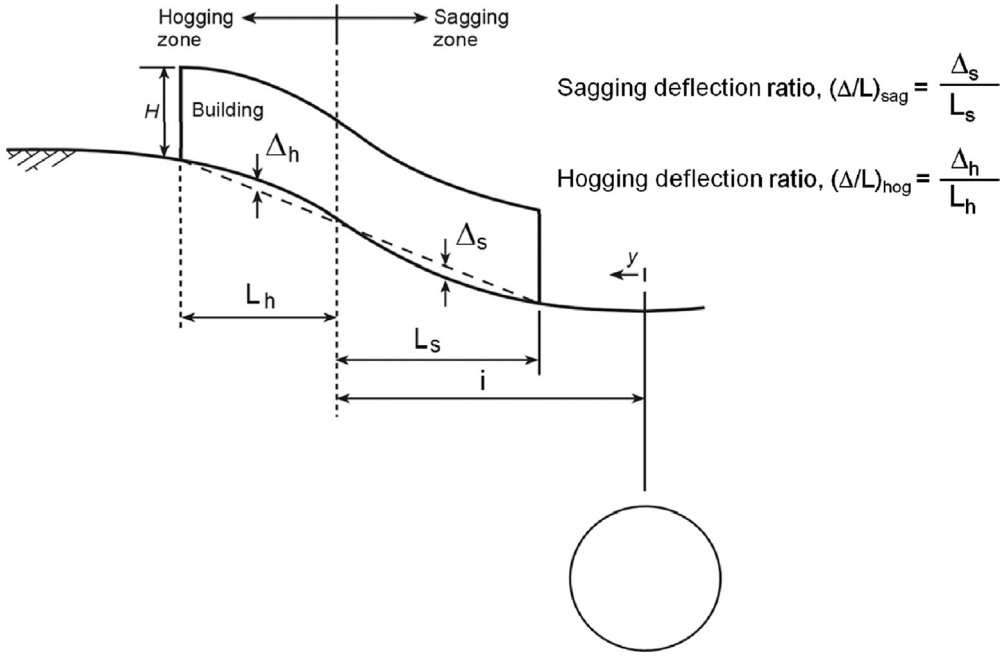

Fig. 1. Deformation of building above tunnelling (after Mair et al., 1996)

the influence of building stiffness, Potts and Addenbrooke (1997) pioneered the use of the modification factor approach to estimate the deflection ratios and horizontal strains caused by tunnelling deformations. In their finite element study, a building was modelled as an elastic beam with bending and axial stiffness properties, and was in full contact with the ground surface. By changing the building's geometry and location or eccentricity in relation to the tunnel, design charts were developed so that the influence of the building stiffness in modifying the response from that of the *greenfield* condition could be estimated.

The use of an elastic beam to estimate a building's stiffness would be appropriate if the building response were dominated by the wall behaviour, such as the masonry houses at Moodkee Street in London, described by Mair and Taylor (2001b). However, it is unclear how the stiffness of framed buildings can be related to the elastic properties of a simple beam. For example, when estimating the realistic bending stiffness of buildings up to 5-storeys for their numerical study, Potts and Addenbrooke (1997) employed the parallel axis theorem to define the stiffness in bending about the neutral axis for a rigidly framed structure, namely,

$$EI_{frame} = \sum E*(I + AH^2)_{\text{ith } floor} \quad (1)$$

Essentially, the stiffness of the 'beam' increases depending on the distance H between the beam's neutral axis and the structure's defined neutral axis, similar to that of composite materials. Nevertheless, Potts and Addenbrooke acknowledged this to be an overestimate of building stiffness. On the other hand, in Mair and Taylor (2001a)'s estimate for the bending stiffness of Elizabeth House, a 10-storey reinforced concrete frame structure with two basement levels, the influence of the frame action was ignored as the effects of any shear walls or moment connections were judged to be minor. The building stiffness was estimated for the 'Class A' prediction (Lambe 1973) by algebraically summing the individual bending stiffness of all the floor slabs, so that

$$EI_{frame} = \sum (EI)_{\text{ith } floor} \quad (2)$$

It is not clear which method would give a better estimate of the bending stiffness of frame structures (although the approach by Mair and Taylor in the case of Elizabeth House led to the Class A prediction being in close agreement with the subsequent field measurements). Moreover, previous studies have been based on buildings on continuous footings that are in full contact with the ground. Using a centrifuge modelling of a simple frame model on separate footings behind an excavation supported by a cantilever wall, Elshafie (2008) observed the beam dislodging from the column-footing due to ground movements during the excavation. The behaviour of framed buildings on individual footings could be quite different from that of a simple beam model.

1.2. Building modification factor approach

The building modification factor approach introduced by Potts and Addenbrooke (1997), which will be used in this paper, is a valuable tool for studying the response of buildings. Essentially, building modification factors describe the maximum deflection ratios and horizontal strains in a building in relation to the *greenfield* condition. The definition of deflection ratio (Δ/L) is given in Fig. 1. To calculate the deflection ratio modification factors, the following steps are undertaken: (i) the deflection ratios are calculated in the sagging and hogging zones corresponding to the building's geometry and location using the *greenfield* settlement trough, i.e., $(\Delta/L)_{sag,GF}$ and $(\Delta/L)_{hog,GF}$; (ii) for the settlement trough for the building

predicted by the FE analysis (influenced by the stiffness of the building), deflection ratios are calculated for the sagging and hogging zones, i.e., $(\Delta/L)_{sag,Bldg}$ and $(\Delta/L)_{hog,Bldg}$; (iii) the modification factors for the deflection ratio (M^{DRsag}; M^{DRhog}) are then calculated by dividing the calculated deflection ratio for the building ($\Delta/L_{sag,Bldg}$; $\Delta/L_{hog,Bldg}$) by the deflection ratio for the *greenfield* settlement trough ($\Delta/L_{sag,GF}$; $\Delta/L_{hog,GF}$):

$$M^{DRsag} = \frac{(\Delta/L)_{sag,Bldg}}{(\Delta/L)_{sag,GF}} \tag{3}$$

$$M^{DRhog} = \frac{(\Delta/L)_{hog,Bldg}}{(\Delta/L)_{hog,GF}} \tag{4}$$

In terms of horizontal strains, the maximum compressive and tensile horizontal strains in the greenfield, corresponding to the building's geometry ($\varepsilon_{hc,GF}$; $\varepsilon_{ht,GF}$), are calculated together with the maximum horizontal strains induced in the building ($\varepsilon_{hc,Bldg}$; $\varepsilon_{ht,Bldg}$). It should be noted that the use of the maximum horizontal strains is different from the use of the average horizontal strains in the procedure for the building damage assessment outlined by Mair et al. (1996). The modification factors for the maximum horizontal strains ($M^{\varepsilon hc}$; $M^{\varepsilon ht}$) are defined as follows:

$$M^{\varepsilon hc} = \frac{\varepsilon_{hc,Bldg}}{\varepsilon_{hc,GF}} \tag{5}$$

$$M^{\varepsilon ht} = \frac{\varepsilon_{ht,Bldg}}{\varepsilon_{ht,GF}} \tag{6}$$

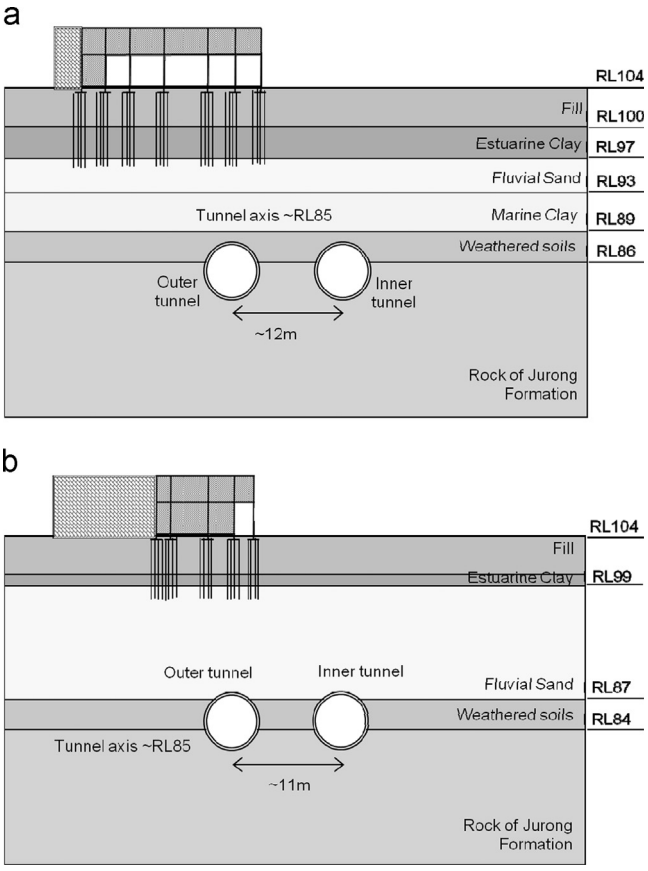

Fig. 2. Cross-sections of the shop houses and soil profiles (a) Near west end of shop house A29 and (b) Near west end of shop house A32.

2. Case study of the response of framed buildings during tunnelling

Goh and Mair (2011a) presented a case study of two framed buildings that were recently subjected to the effects of twin bored tunnelling drives along Pasir Panjang Road in Singapore. These buildings, or shop houses as they are referred to, are two-storey reinforced-concrete framed buildings whose columns are founded on individual footings supported by short timber bakau piles (estimated to be from 6 m to 9 m long). At the ground floor, there are tie-beams connecting the main columns of the frame, but not all columns are connected in both directions. In particular, the columns along the 'five-foot way' – a five-foot wide common corridor running along the front of the building – are unconnected at the ground floor level. At the first floor, the beams connect all the columns together (including the columns above the five-foot way) in a grid as they transfer the loads from the first floor slabs down to the foundation. The slabs are 100-mm thick and the building façade and internal walls are mostly formed using brick in-fills. Fig. 2 shows the cross section of the two shop houses in relation to the twin bored tunnels. The bored tunnelling was undertaken using earth-pressure balance shield machines (Venkta et al., 2008), and whilst the first (inner) tunnel was constructed away from the shop houses, the second (outer) tunnel was constructed directly below the shop houses. The depths to the tunnel axis ranged from 16 m to 19 m below the ground surface, and the bored tunnels were constructed in a mixed face condition of the Kallang Formation (whose members are soft clays and sands of fluvial and marine origin; Tan et al., 2003) and the Jurong Formation (whose members are mud-stones, siltstones, and sandstones of sedimentary origin and exhibiting evidence of metamorphism; Leong et al., 2003).

A detailed instrumentation programme was implemented during the bored tunnelling works, including settlement measurements of the building and tape extensometer measurements between the columns. Fig. 3 shows one of the monitored building settlement arrays compared with the settlement profile in the greenfield condition. Based on the monitored ground settlement markers at this location, the back-analysed volume loss was 1.3% during the first tunnel drive. A narrow trough width for the Gaussian settlement curve provided a good match to the building settlement behaviour during the first tunnel drive (Fig. 3a). The trough width (i) of a Gaussian settlement curve is related to the depth to tunnel axis (z) and trough width parameter K, where $i = K*z$. Based on field data compiled by Mair and Taylor (1997), the surface trough width parameter for tunnelling in sands would vary between 0.25 and 0.45 with an average value of 0.35. Furthermore, Mair et al. (1993) proposed a sub-surface trough width parameter which decreases when the subsurface trough is nearer to the tunnel axis. The combined effects of tunnelling in fluvial sand and the building settlement occurring at a depth nearer to the toe levels of the piles, resulted in the narrow settlement trough width observed in this case study. However, using the same trough width parameter for the

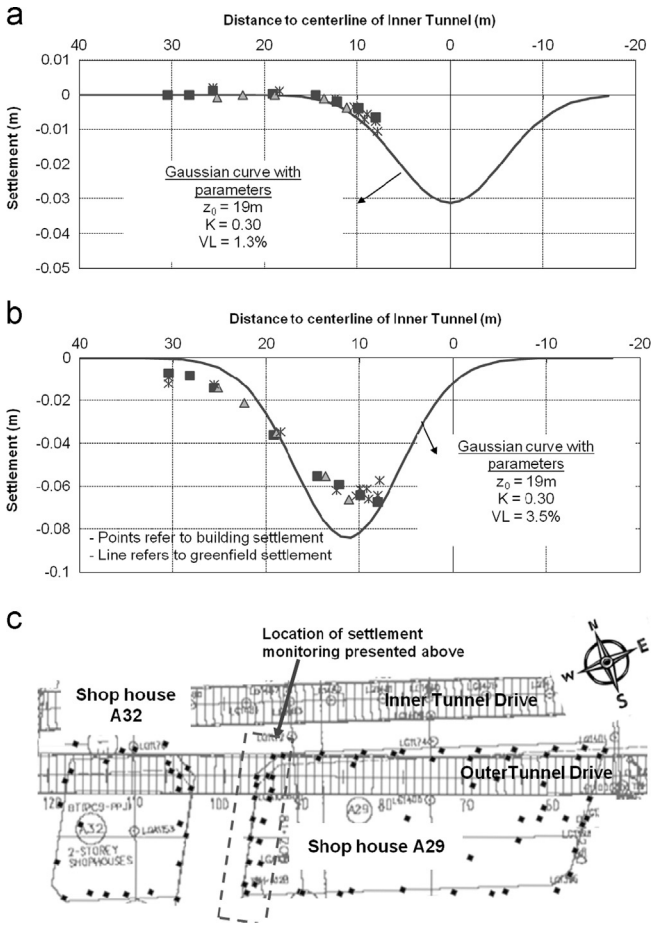

Fig. 3. Greenfield and building settlement at west end of shop house A29 (a) Settlement due to inner tunnel drive, (b) Settlement due to outer tunnel drive and (c) Layout of building settlement markers.

second tunnel drive (as seen in Fig. 3b), the building would be in the sagging deformation region directly above the tunnel and in the hogging deformation region further away from the tunnel. The volume loss also increased to 3.5% during the second tunnel drive. Moreover, it was noted that the settlement response of the building during the second tunnel drive is semi-rigid compared to the *greenfield* settlement trough. This is in contrast to the flexible behaviour when the building is in a purely hogging mode during the first tunnel drive. Furthermore, the maximum building settlements due to the first and second tunnel drives were 10 mm and 67 mm, respectively. Although the shop houses had settled substantially due to both tunnel drives, building inspections showed that there was no structural distress either during or after the tunnelling. Liew et al. (2008) reported that the induced crack widths in the building ranged from 0.3 mm to 1.5 mm, except for an isolated location registering 9.8 mm at an end wall. This would have placed the building in the 'slight' damage category using the guidance on damage classification by the Building Research Establishment (BRE Digest 251). This is attributed to the building damage being caused by distortion (and measured indirectly using deflection ratios) rather than absolute displacement. This case study illustrates the beneficial effect of the framing action by columns and beams in reducing the deflection ratio and building damage.

Another interesting aspect of this case study is the horizontal strains monitored using tape extensometers between the columns. As reported by Goh and Mair (2011a), horizontal strains were low during the first tunnel drive due to the inner tunnel being further away from the buildings, but these became significant during the second tunnel drive when the outer tunnel was directly below the buildings. It was also reported that horizontal strains longitudinal to the tunnel were generally low, and horizontal strains were more significant in the transverse direction to tunnelling. Fig. 4 shows the transverse horizontal strains monitored in one of the buildings, where the building strains may be compressive or tensile in nature depending on the location with respect to the settlement curve caused by the tunnelling. This figure also illustrates that the horizontal strains in buildings on individual footings may be very significant (up to a maximum value of 0.24%), which is in contrast to previous case studies of buildings on continuous footings where monitored horizontal strains were generally negligible (such as the case of the Moodkee Street buildings reported by Dimmock and Mair, 2008). It is further noted that the highest horizontal strains occur between columns that are unconnected at the ground floor level (maximum of 0.24% in TEX1148) and mostly along the five-foot way area. For columns that are connected by ground beams, the horizontal strains are much lower (maximum of 0.08% in TEX1144). This finding suggests some influence from the framing action on the horizontal strain behaviour of buildings.

To understand the influence of the frame action on building stiffness, Goh (2010) conducted a numerical study using the finite element method to investigate the response of framed structures to movements caused by multi-propped excavations in soft clays. The buildings were modelled using a structure frame in a 2D plane analysis – first with a continuous footing perpendicular to the excavation, and then with separate individual column footings. The response of the frame models was compared with another set of finite element models where the building was modelled using an elastic beam. From the structural analysis, parameters describing the influence of the frame action were derived and an approach describing its influence on the response to excavation-induced deformations was presented. The subsequent sections of this paper summarise the findings of the study.

3. Frame structures on continuous footings

3.1. Finite element model study

An effective stress, plane strain analysis was carried out using the finite element software Abaqus, where a braced excavation was simulated near a building. The excavation is in soft clay, assuming undrained conditions, and was supported using a multi-propped retaining wall with adequate toe embedment into stiff clay. Fig. 5 shows the key elements in the base model of the analysis (model UD_A), where a 20-m-deep excavation was simulated in a 20-m-thick deposit of soft clay and the buildings were modelled first as an elastic beam (Fig. 5a) and then using a structural frame (Fig. 5b). A 0.8-m-thick diaphragm

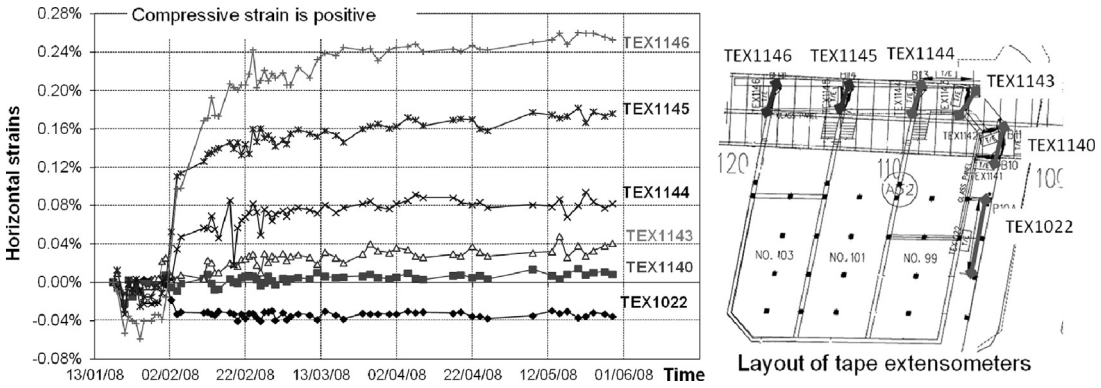

Fig. 4. Development of transverse horizontal strains during second tunnel drive in shop house A32.

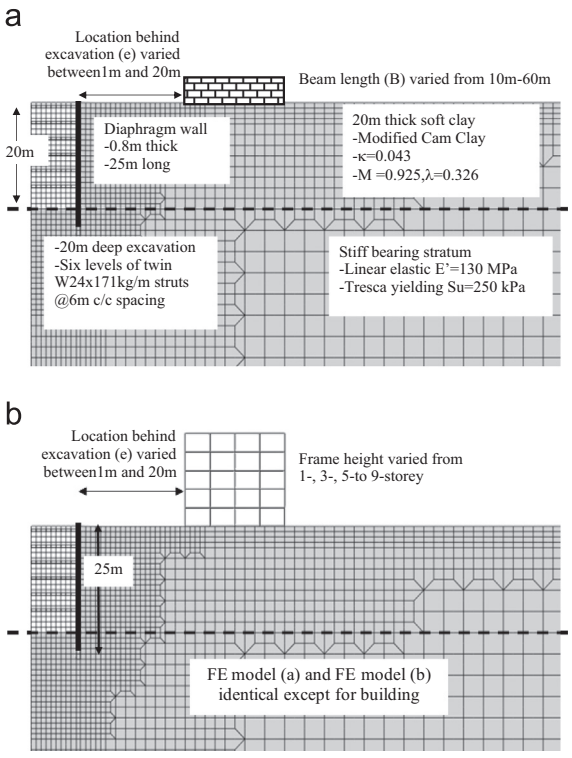

Fig. 5. Excavation configuration and soil parameters in the finite element study. (a) Key elements of base model of analysis and 'simple beam' building and (b) Model of a frame structure building on continuous footings.

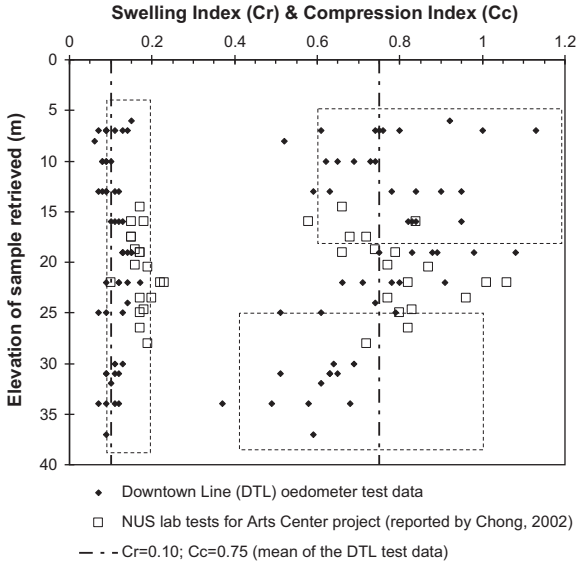

Fig. 6. Oedometer test data of the Singapore Marine clay.

wall was modelled in the excavation with a Young's modulus of 1.89×10^7 kN/m^2 corresponding to that of a cracked section and in line with recommendations in the CIRIA report C580 for embedded retaining walls. The soft clay was modelled using the Modified Cam-Clay model, and the stiff underlying stratum – mainly for the purpose of ensuring proper embedment of the wall toe – was modelled using a linear elastic, perfectly plastic soil model with Tresca yielding. The parameters for the soft clay were taken from the recent soil investigation works carried out on Marine Clay for the new Downtown Line project in Singapore (see Fig. 6). In particular, the mean swelling and compression indices of the Singapore Marine Clay investigated in the Downtown Line project were found to be comparable to the oedometer test results by Tanaka et al. (2001) and Chong (2002), as shown in Fig. 7.

Table 1 summarises the key soil parameters used in the base excavation model.

The building was first modelled as a weightless, elastic beam with axial and bending stiffness properties, similar to the elastic beam simplification used in the study by Potts and Addenbrooke (1997) for buildings under the influence of tunnelling-induced deformations. The axial stiffness and bending stiffness of the elastic beam were varied as shown in Table 2. The bending and axial stiffness of a building depends not only on the wall thickness, but also on the slab thickness, the frame action, the wall openings, etc. There may be times when the bending and the axial stiffness are the same, but there are also many more occasions of other stiffness combinations for various buildings. A parametric study conducted by Goh (2010) on simple beam buildings found that the horizontal response of a building is independent of its bending stiffness, whilst its settlement response is independent of its axial stiffness in the realistic range. Hence, a range in axial and bending stiffness was selected which would give a complete range in modification factors, rather than represent the specific building configurations.

Next, frame models of various heights, also weightless and up to 9-storeys, were simulated for which the beams and the

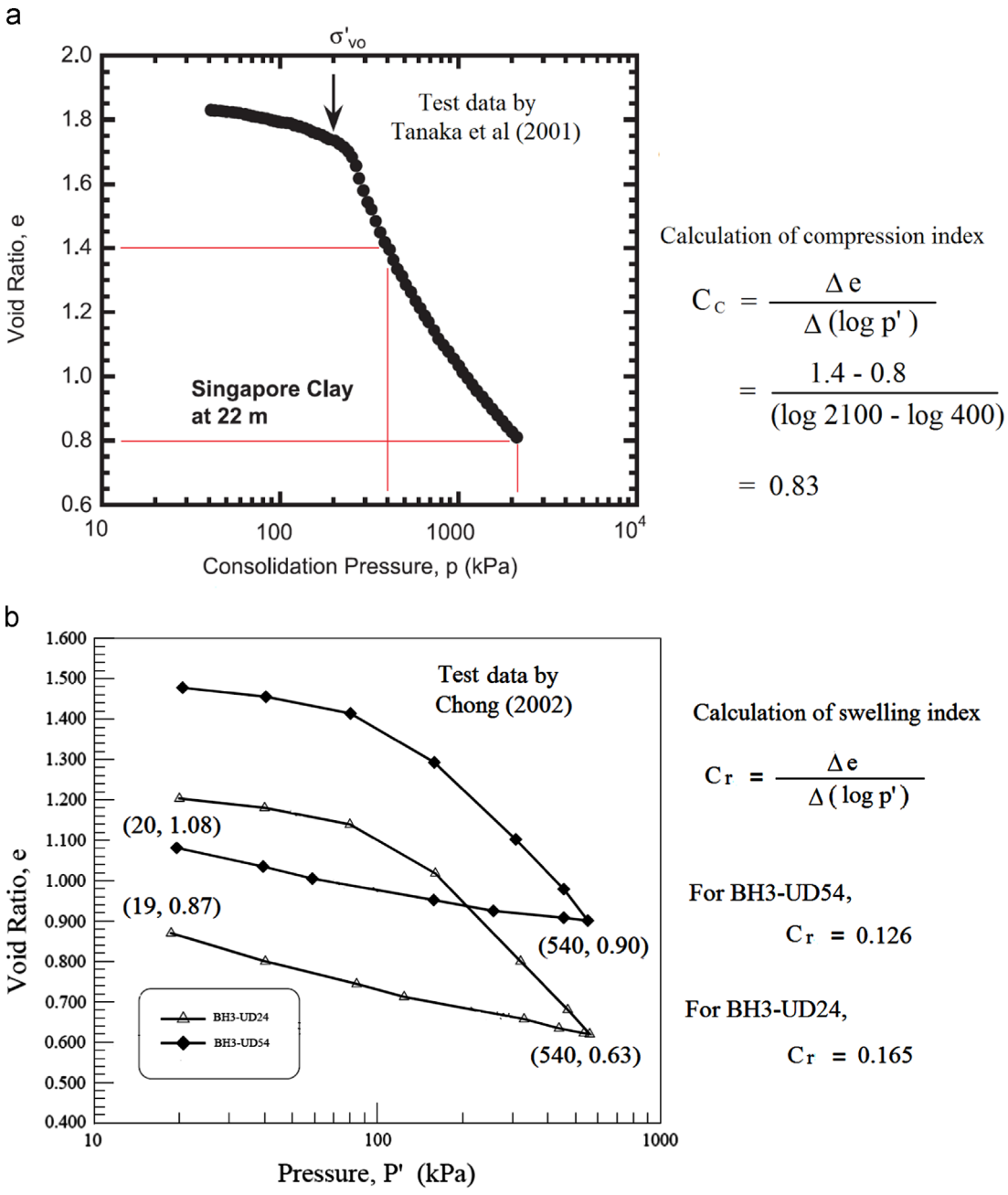

Fig. 7. Analysis of oedometer test data by (a) Tanaka et al. (2001) and (b) Chong (2002) on Singapore marine clay.

Table 1
Soil parameters used in finite element model.

Soil stratigraphy	Constitutive model	Soil parameters
20 m thick soft clay	Modified Cam-Clay (porous elastic)	$\nu'=0.2$; $\kappa=0.10$ / ln10=0.043
	Modified Cam-Clay (clay plasticity)	M=0.925; $\lambda=0.75$ / ln 10=0.326
Underlying stiff soil	Linear elastic	$\nu'=0.3$; E'=0.87*Eu=130000 kPa
	Perfectly plastic (Mohr Coulomb)	c'= Su=250 kPa; $\phi'=0^\circ$; $\psi'=0^\circ$

Table 2
Combination of stiffness for simple beam models.

Elastic beam	#1	#2	#3	#4	#5	#6
Bending stiffness EI (kNm^2 per metre run)	10^3	10^4	10^5	10^6	10^7	10^8
Axial stiffness EA (kN per metre run)	10^3	10^4	10^5	10^6	10^7	10^8

columns were rigidly connected to the column elements. The lengths (B) and the distances of the frame models behind the excavation (e) were the same as the simple beam models;

Table 3
Configurations of rigidly framed models for comparison with simple beam models.

ID	Raft thickness	Beam thickness	Beam length per bay	Floor height	Column type
	$B=20$ m, $e=1$ m; $B=20$ m, $e=20$ m				
Base	500 mm	250 mm	5 m	3.5 m	150 mm RC wall
FB	250 mm	100 mm	5 m	3.5 m	
LB	500 mm	250 mm	10 m	3.5 m	
TC	500 mm	250 mm	5 m	5 m	
FBC	250 mm	100 mm	5 mm	3.5 m	150 × 150 RC
SF	250 mm	100 mm	10 m	5 m	columns@5 m
	$B=40$ m, $e=20$ m				
Base	500 mm	250 mm	5 m	3.5 m	150 mm RC wall
FB	250 mm	100 mm	5 m	3.5 m	
FBC	250 mm	100 mm	5 m	3.5 m	150 × 150 RC
	$B=60$ m, $e=20$ m				
Base	500 mm	250 mm	5 m	3.5 m	150 mm RC wall
FB	250 mm	100 mm	5 m	3.5 m	
TC	250 mm	100 mm	10 m	5 m	
FBC	250 mm	100 mm	5 m	3.5 m	150 × 150 RC
	$B=60$ m, $e=1$ m				
Base	500 mm	250 mm	5 m	3.5 m	150 mm RC wall
FB	250 mm	100 mm	5 m	3.5 m	
TC	500 mm	250 mm	5 m	5 m	
LB	500 mm	250 mm	10 m	3.5 m	
FC	500 mm	250 mm	5 m	3.5 m	150 × 150 RC
	$B=40$ m, $e=1$ m				
Base	500 mm	250 mm	5 m	3.5 m	150 mm RC wall
FB	250 mm	100 mm	5 m	3.5 m	
FBC	250 mm	100 mm	5 m	3.5 m	150 × 150 RC

they were selected to yield a mix of sagging and hogging deformation behaviour, as shown below:

- Buildings in sagging deformation only: $\{B=20$ m, $e=1$ m$\}$
- Buildings in hogging deformation only: $\{B=20$ m, $e=20$ m$\}$, $\{B=40$ m, $e=20$ m$\}$, $\{B=60$ m, $e=20$ m$\}$
- Buildings in both sagging and hogging deformation modes: $\{B=40$ m, $e=1$ m$\}$, $\{B=60$ m, $e=1$ m$\}$

Table 3 shows the configurations of the modelled frame structures. Similar to the simple beam models, the frame models were weightless. A no-separation criterion was defined at the interface between the soil and the building. Interface sliding was allowed between the buildings and the soil, and this was simulated using a friction model for which the contact surfaces were allowed to carry shear stresses up to 20 kPa (which is in the range of the undrained shear strength of Singapore Marine Clay at shallow depths) before they slid relative to one another. Defining a "no separation" criterion together with the friction model allows the soil–structure contact pair to slide relative to each other, but not to separate perpendicular to the contact. This ensures that the horizontal displacement of the building is not constrained or underestimated.

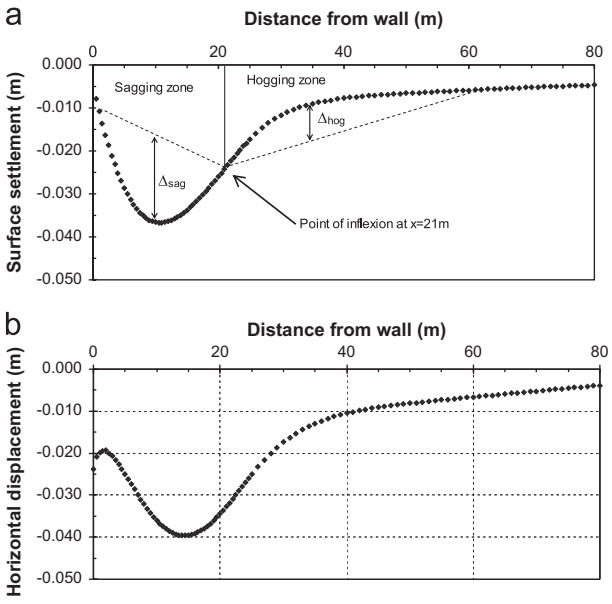

Fig. 8. Surface settlement and horizontal displacement profiles in greenfield condition.

3.2. Effect of bending and axial stiffness on building deformation

To determine the deflection ratio in the building and in the *greenfield* condition, the sagging and hogging zones of the settlement curve were obtained by interrogating for the inflexion point – or the point of maximum slope – on the building and the ground settlement profiles, respectively. Fig. 8 shows the surface settlement and horizontal displacement profiles in the *greenfield* condition for the excavation simulated in base model UD_A. It illustrates the inflexion point that separates the surface displacement profile into a sagging zone and a hogging zone. The sagging zone of the surface settlement trough extended to 21 m behind the excavation.

3.3. Settlement behaviour of simple beam models compared to frame models

To compare the settlement behaviour of the simple beam models with the frame models, modification factors for the deflection ratio were calculated and plotted against the bending stiffness of the building. The bending stiffness of the buildings in the simple beam model is simply the bending stiffness of the elastic beam. For the frame structure models, estimates of the bending stiffness were made using Eq. (1) and Eq. (2) separately.

Fig. 9 shows the variation in deflection ratio modification factors with bending stiffness for the 20-m building when it is 1 m behind the excavation ($e=1$ m, sagging deformation only) and when it is 20 m behind the excavation ($e=20$ m, hogging deformation only), using both methods to estimate the frame stiffness. The modification factors from the frame structure models with various configurations are shown as points, whilst those from the simple beam models are plotted as a curve. For both modes of deformation, when the frame stiffness is

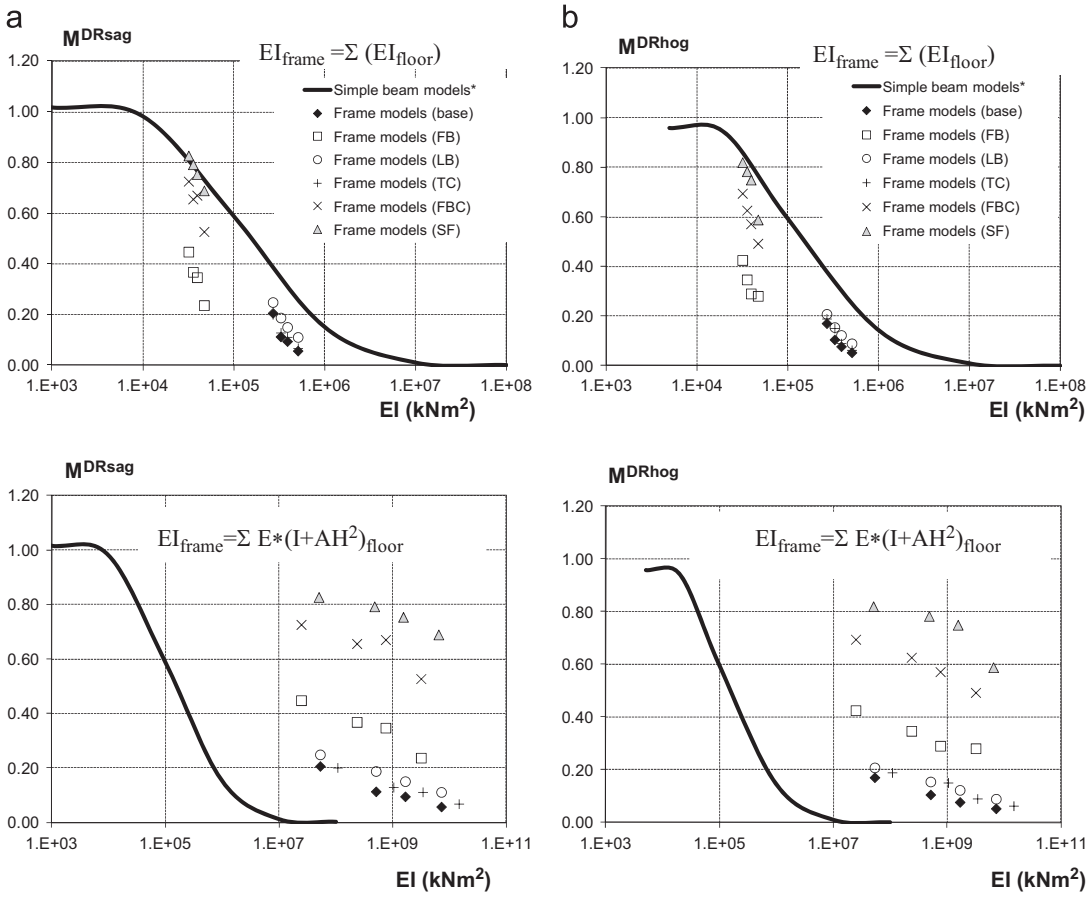

Fig. 9. Deflection ratio modification factors for bending stiffness estimated using different methods. (a) For 20m long buildings with e=1m and (b) For 20m long buildings with e=20m.

estimated by summing the bending stiffness of each floor slab (using Eq. (2)), the results are all below the curves from the simple beam models. This suggests that simply summing the bending stiffness of each floor slab will result in a lower estimate of the frame stiffness when compared to that of the simple beam. However, when the frame stiffness is estimated by increasing the contribution of bending stiffness of each floor slab, according to the parallel axis theorem (using Eq. (1)), the results are seen to plot above the curves derived from the simple beam models. This approach results in a higher estimate of the bending stiffness of a rigidly connected frame structure in relation to the simple beam.

3.4. Stiffening influence of columns on beams

Meyerhof (1953) obtained an approximate estimate of the flexural rigidity of a rigidly framed structure. He considered an open multi-storey building frame with approximately equal bays and deflecting into the shape of a trough with a maximum central deflection and with similar curvature at each floor level. By assuming points of contra-flexure in the columns at its mid-storey height and solving the structural analysis equations, he showed that the effect of the columns in rigidly connected frame structures is the increase in flexural rigidity of the entire beam line by a column stiffening factor.

Following Meyerhof's assumed structural mode of deformation, a column stiffening factor C can be derived using slope deflection equations (Goh 2010); it is defined with slight changes to its terms as follows:

$$C = \left[1 + \frac{L^2}{l^2}\left(\frac{K_{LC}+K_{UC}}{K_{LC}+K_{UC}+K_B}\right)\right] \tag{7}$$

where L is the length of the beam line in sagging or in hogging, l is the span length of each beam bay, $K_{LC}=(EI/h)_{LC}$ is the average stiffness of the lower column, $K_{UC}=(EI/h)_{UC}$ is the average stiffness of the upper column, and $K_B=(EI/l)_B$ is the average stiffness of the beam line. The bending stiffness of the frame structure can then be written as follows

$$EI_{frame} = \sum(EI^*C)_{ithfloor} \tag{8}$$

The suitability of the column stiffening factor in estimating frame stiffness can be illustrated by plotting the modification factors of the frame structure models against the factors of the simple beam models, as shown in Fig. 10. When the bending stiffness of the same frames plotted in Fig. 9 was estimated using the column stiffening factor, the estimated frame stiffness coincided with the bending stiffness of the simple beam models for the same modification factor. When longer frame structures were modelled, the modification factor plots show a similar match in frame stiffness with the corresponding

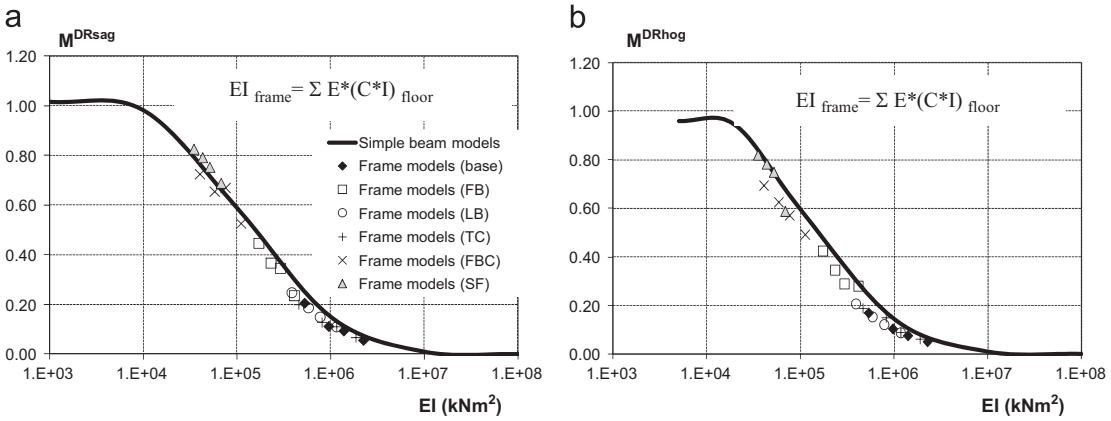

Fig. 10. Deflection ratio modification factors for bending stiffness estimated using the column stiffening factor. (a) For 20m long buildings with e=1m and (b) For 20m long buildings with e=20m.

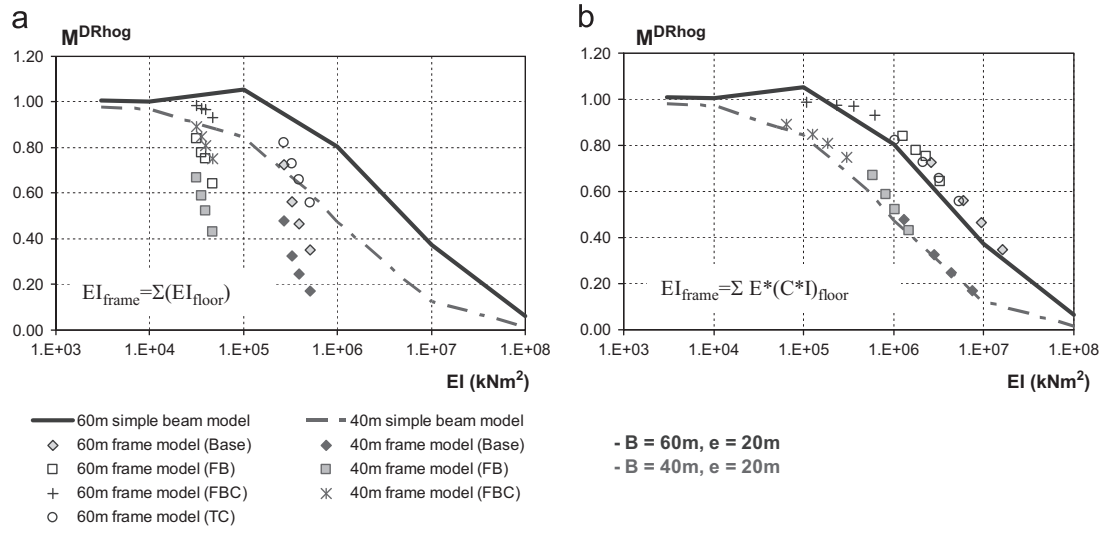

Fig. 11. Modification factors for longer frames under hogging deformation

Table 4
Variation of composite frame structure models for 20 m buildings (e=1 m, 20 m).

Identifier	Base	LB	TC	FB	FBC	SF	SC
Beam type	H610 × 305 × 149 kg/m @5 m spacing (E=205 GPa, I=1.259 × 10^{-3} m^4)			H457 × 191 × 98 kg/m @ 5 m spacing (E=205 GPa, I=4.573 × 10^{-4} m^4)			
RC raft thickness	500 mm	500 mm	500 mm	500 mm	250 mm	250 mm	250 mm
Bay length	5 m	10 m	5 m	5 m	5 m	10 m	5 m
Column height	3.5 m	3.5 m	5 m	3.5 m	3.5 m	5 m	3.5 m
RC column type	150 mm walls				200 × 200 mm @5 m spacing		300 mm walls

simple beam model when the column stiffening factor is used (Fig. 11).

3.5. Modifications to the column stiffening factor

In the original formulation, Meyerhof had considered frame structures where the beam and the columns were of the same material. In the derivation presented by Goh (2010), however, the Young's modulus of the material was included so that the stiffness of frame buildings with different column and beam materials may be estimated using the column stiffening factor. To check the formulation, 1-storey and 5-storey frame structures of steel beams on RC columns were modelled for 20-m-long buildings located 1 m and 20 m behind the excavation. Table 4 shows the variation in structural elements modelled, where the beams were made of steel and the columns were reinforced concrete. The modification factor curves of the frame models, matching the simple beam models (Fig. 12), show that the column stiffening factor is adequate even when the columns and beams are made of different materials.

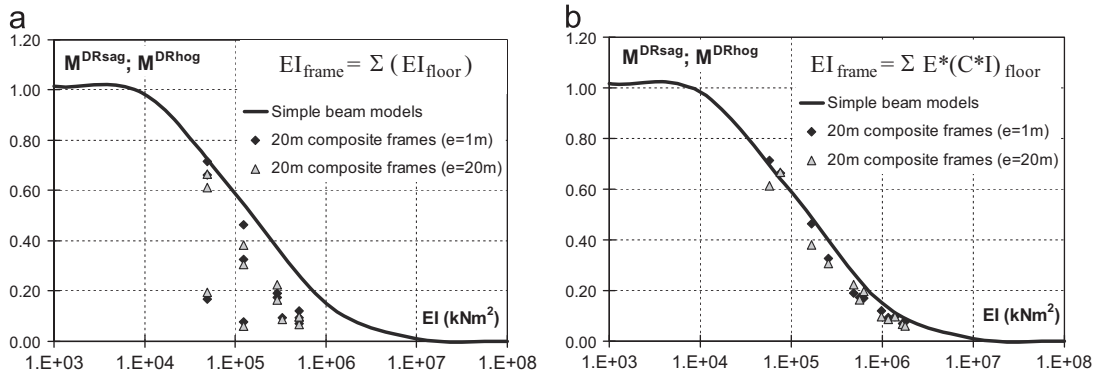

Fig. 12. Modification factors for buildings with different materials.

The derivation of the column stiffening factor was based on the frame structure deflecting in a sagging deformation mode. This has to be modified for buildings showing both sagging and hogging deformation modes behind an excavation. It is suggested that length L in the column stiffening factor Eq. (7) be defined as the sagging length and the hogging length of the building in the *greenfield* settlement trough, instead of the whole length of the building. This can be checked by analysing the frame models that are longer than the sagging length of the surface settlement trough, such as the 60-m- and 40- m-long frame buildings located 1 m behind the excavation. Fig. 13 shows the modification factor plots of these frame models in double deformation modes compared to the simple beam models. With a slight modification to the definition of beam length, the column stiffening factor can still provide a good estimate of the bending stiffness even for framed buildings that are in part sagging and in part hogging deformation.

3.6. Frames with pinned structural connections

Not all frame structures are made of rigidly connected beams and columns. Some buildings may consist of pin-connected frames, where the beams are simply supported by columns and are not restrained by the columns in their bending. Some examples are buildings constructed using precast elements where the precast beams are placed on the corbels of columns, and also the simple construction technique where in steel frames the I-beams are bolted only on its web and not on its flange to the columns. Lateral stability of the frame will likely be provided by bracing or shear walls in other parts of the building. In general, two cases can be considered. They are shown in the schematic in Fig. 14.

The first case is when the beams are pinned to the columns and are unconnected between adjacent bays, such as the simple steel frame construction and the precast beams on column corbels. There would be no contribution by the beams to the bending stiffness of the frame structure when they are hinged between columns. As such, the column stiffening factor would be zero so that the bending stiffness for such buildings would derive only from their foundation.

The second case occurs when the columns do not restrain the beams in bending, but the beams are continuous within the floor level, such as in flat slab systems and also for floor slabs in a typical building. The beam would deflect according to its own bending stiffness without any stiffening effect from the columns. In this case, the continuous beam still contributes to the overall frame stiffness with a column stiffening factor of unity. Fig. 15 shows the modification factors from the finite element models of a frame with beams that are simply supported on the columns compared to the simple beam models. The frame stiffness would be well-estimated using Eq. (2) (equivalent to Eq. (8) with $C=1$).

3.7. Horizontal strains

Fig. 16 plots the modification factor of horizontal strains against the axial stiffness of the buildings for the frame models in comparison to the simple beam models. For all the frame buildings on continuous footings, the horizontal strains are negligible. This is in part due to the interface sliding allowed between the soil and the structure elements in the finite element models. The sliding of the soil underneath continuous footings behind the excavation has been observed by Elshafie (2008) in his centrifuge model experiments. More importantly, the high axial stiffness of realistic buildings limits the development of axial strains for buildings on continuous footings. Even with just a 100-mm-thick RC slab, the axial stiffness of a continuous footing would be 2×10^6 kN. This may also be inferred from the design charts by Potts and Addenbrooke (1997), who used a non-slipping interface between the soil and the building, and where the maximum horizontal strain modification factors were less than 0.10.

So far, the discussions have been about buildings on continuous footings. Mair (2003) pointed out that horizontal strains induced in most buildings are usually reduced significantly, based on field case histories, but this may not be true for buildings on individual footings. The next section presents a study on frame structures on individual footings.

4. Frame structures on individual footings

4.1. Settlement behaviour and modification factors of deflection ratio

Finite element models were made of frame structures on individual footings separated at the ground level. These frame models were subjected to the same ground and excavation

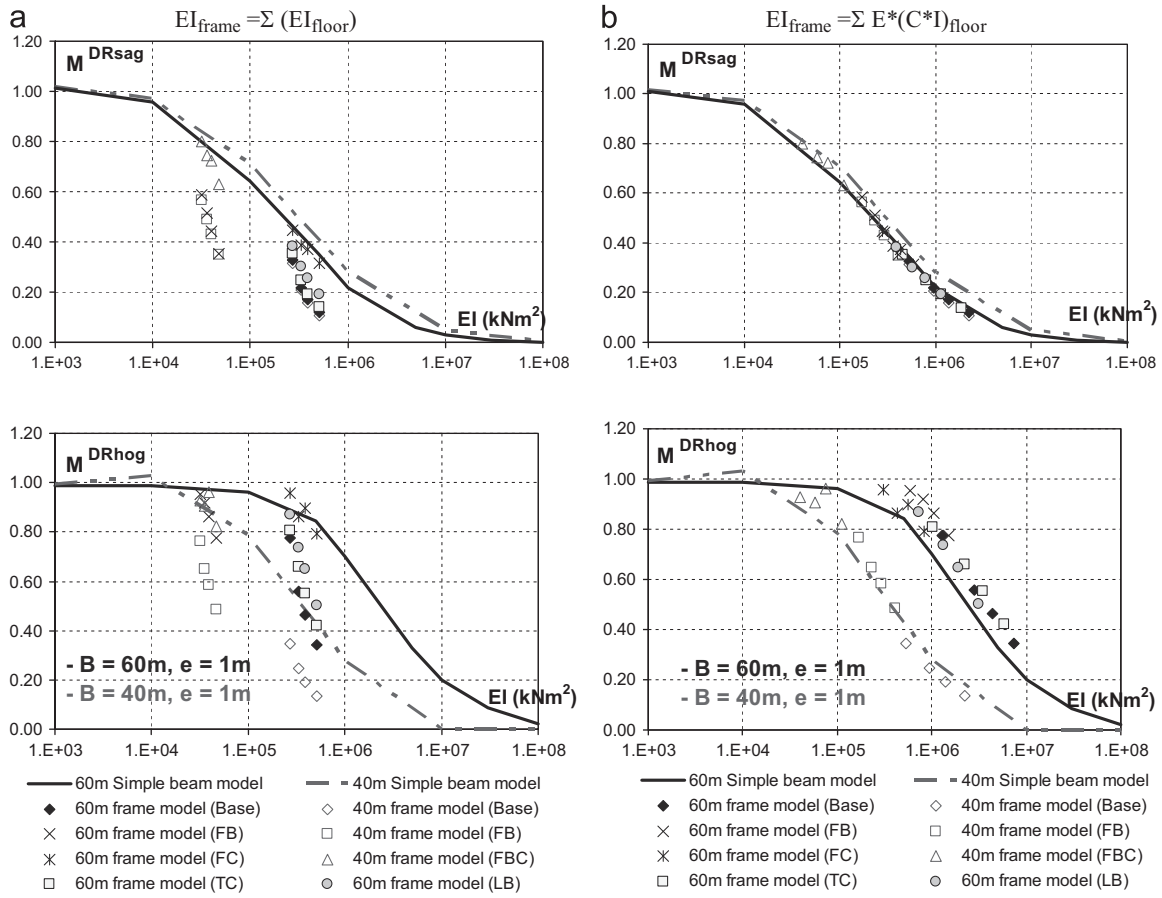

Fig. 13. Deflection ratio modification factors for buildings in both sagging and hogging deformations.

conditions corresponding to base model UD_A. Fig. 17 gives an overview of the frame structures modelled in this study. 20-m- and 60-m-long frame structures were modelled at $e = 1$ m and $e = 20$ m behind the excavation. The frames were 2-storeys and 10-storeys high for the 60-m-long buildings, and 10-storeys high for the 20-m-long buildings. The variation in column and beam types for the frame structures is summarised in Table 5. As with the frames on continuous footings, horizontal sliding was allowed between the soil and footing elements at the interface, but no separation was specified to ensure that the soil and the footing elements would remain in contact throughout the analysis.

Fig. 18 shows the surface settlement and the horizontal displacement profiles in the greenfield condition and the footing displacement of the frame on individual footings for the case of $e = 1$ m. The response of the footings is more rigid than the ground displacement behaviour in the greenfield condition. As before, the settlement behaviour of frames on individual footings is studied by comparing the modification factors of the deflection ratio for the frame models against those of the elastic beam models. For each frame, the modification factors are plotted against the bending stiffness estimated using Eqs. (2) and (8). Fig. 19 and 20 show modification factor plots for the 20-m- and 60-m-long frames on individual footings. Compared to simply summing the bending stiffness of each individual beam line, the column stiffening factor improves the estimate of the bending stiffness of the frame on individual footings so that its modification factor response is nearer to that of the elastic beam simplification. However, the estimated stiffness of the frames on individual footings is still slightly lower. This could have been caused by the reduced soil–footing contact for the frames on individual footings. Nevertheless, the differences between the modification factor relationships are small. It would be reasonable to use the column stiffening factor to estimate the bending stiffness of the frames on individual footings, and to use the design charts developed using simple beam models to estimate the modification factor and the deflection ratios of the building.

4.2. Horizontal strains

As illustrated in Fig. 18, the *greenfield* horizontal strains are calculated between the locations of the individual footings, whilst the building horizontal strains are calculated between the individual footings of the frame model at the ground floor. Depending on the particular nature of the soil–structure interaction, it was observed that the location of the maximum horizontal strains between the separated footings may not coincide with the location in the greenfield. Moreover, this location of maximum horizontal strains would be different between the various frames modelled in the study. Thus, the

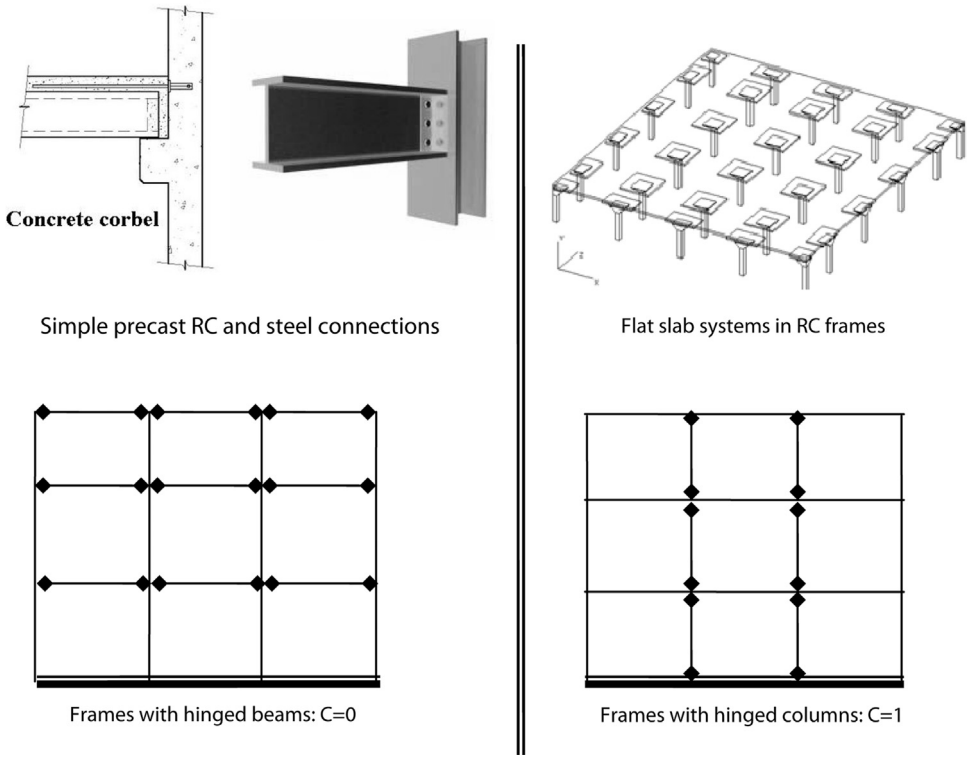

Fig. 14. Types of simply connected frames and their examples

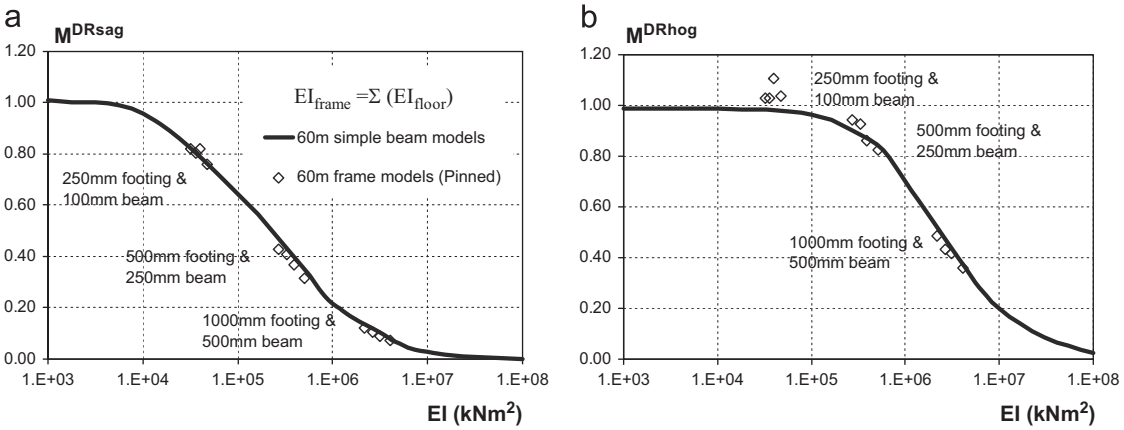

Fig. 15. Deflection ratio modification factors for frames with simply supported and continuous beams.

horizontal strain modification factor was defined based on the maximum of the building horizontal strains divided by the maximum of the *greenfield* horizontal strains. With this definition, the modification factors of maximum compressive strains and maximum tensile strains may be calculated and plotted onto the modification curves for the simple beam model.

As observed in Fig. 21, the horizontal strain modification factors can be substantially higher than those of the simple beam model, and ranged from 0 to 1 irrespective of the axial stiffness. Although the axial stiffness for a framed building may be sufficiently high so that horizontal strains in the building are small, the individual footings could cause significant horizontal strains between columns at the ground floor level. This could then induce significant strains on the slabs at the ground level and is in contrast to the frames on continuous footings for which the modification factors are near to zero. Furthermore, two observations can be made from the frame parameters varied in the study. Firstly, the horizontal strain modification factor ($M^{\varepsilon h}$) decreased as the distance between the footing on the ground level and the first floor tie beam (h) was reduced, from $M^{\varepsilon h} \sim 1$ at $h = 3$ m to $M^{\varepsilon h} \sim 0$ when $h = 0.2$ m. Secondly, the horizontal strain decreased when the column stiffness increased. When the tie-beams were fixed 3 m away from the footing and the ground level, the increase in the column size from 150×150 mm RC

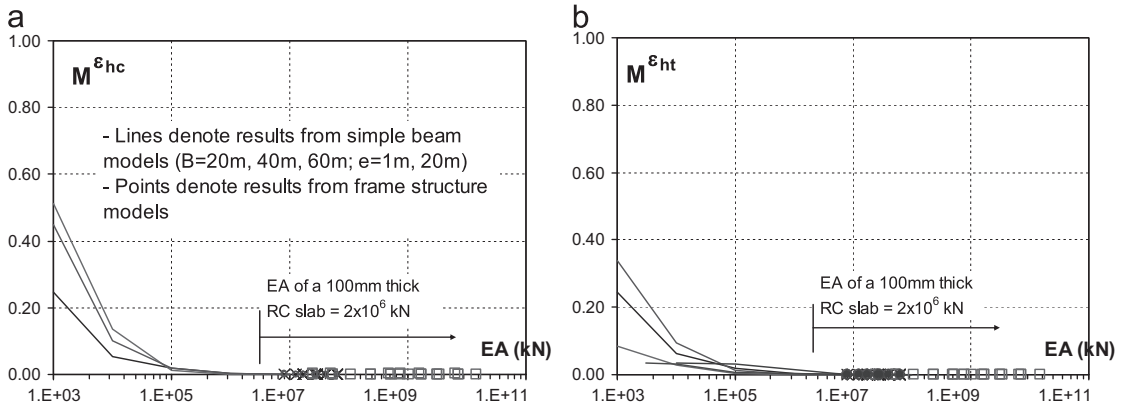

Fig. 16. Horizontal strain modification factors for frames on continuous footings compared to those for simple beam models. (a) Compressive horizontal strain modification factors and (b) Tensile horizontal strain modification factors.

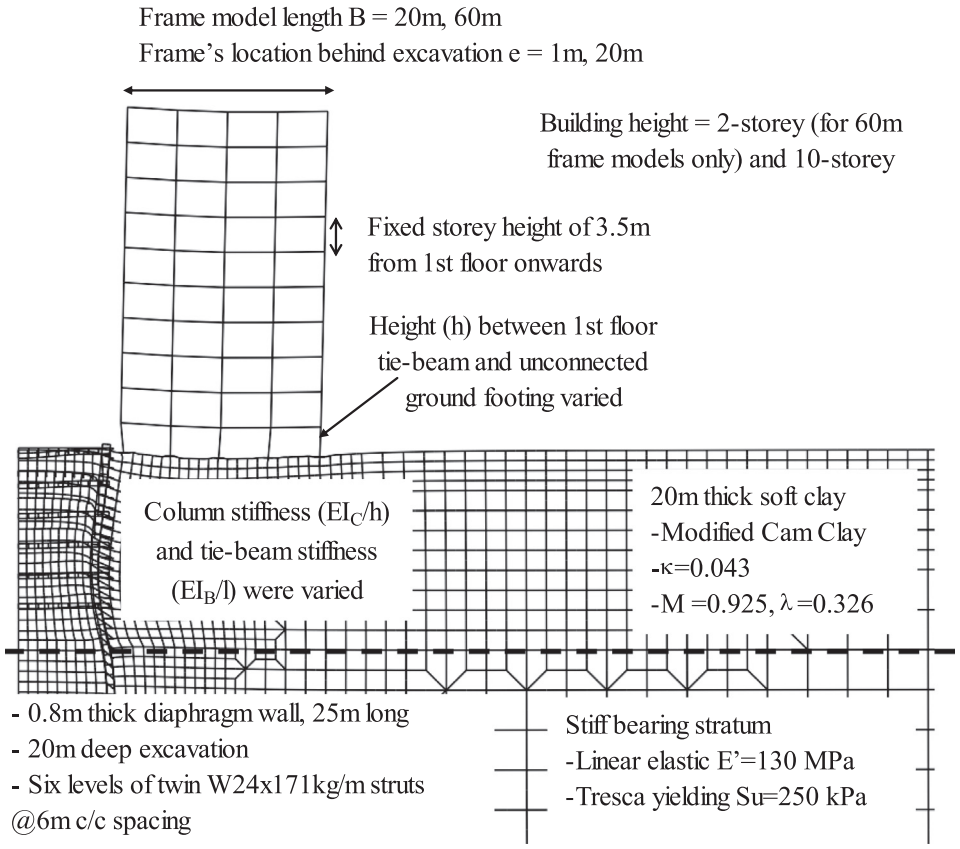

Fig. 17. Excavation model and soil parameters for frames on individual footings.

columns to 150 mm RC walls reduced the M^{eh} from unity to around 0.2. The axial stiffness is less adequate than the frame stiffness in describing the horizontal response of framed buildings on separate footings.

4.3. Frame stiffness factor

A measure of horizontal stiffness for the frame action in the ground floor can be obtained, by determining the force needed to move the support of a structure frame horizontally by a unit displacement. As an approximation, a simple portal frame with a single bay was analysed. As the individual footing is unable to offer much moment restraint to the column in the building frame, the simple portal frame was assumed to be pin-supported. A schematic of this portal frame is shown in Fig. 22. The derivation of the stiffness relationship was done using a structural analysis by the slope deflection method (Goh 2010). A frame stiffness factor (α_f) may thus be defined as

$$\alpha_f = \frac{H}{\Delta} = \frac{3K_B K_C}{h^2(2K_B + 3K_C)} \tag{9}$$

The frame stiffness factor has a dimension of kN/m per metre run; it is dependent on the column height at the ground floor (h) as well as on the bending stiffness of the column (K_C) and the

Table 5
Variation of frame structure models for the 20 m and 60 m long buildings on individual footings.

Beam type	1st floor tie-beam type	Column type	Distance between 1st floor beam and footing
100 mm RC slab, with 5 m bay length	100 mm RC slab	150 × 150 mm RC column @5 m	h=0.2 m, 1 m, 2 m, 3 m
		150 mm RC wall	h=0.2 m, 1 m, 2 m, 3 m
	300 × 300 mm RC beam @5 m	150 × 150 mm RC column @5 m	h=3 m
		100 mm RC wall	h=3 m
	250 mm RC slab	150 × 150 mm RC column @5 m	h=0.2 m, 1 m, 2 m, 3 m
		150 mm RC wall	h=0.2 m, 1 m, 2 m, 3 m
100 mm RC slab, with 10 m bay length	100 mm RC slab	150 × 150 mm RC column @5 m	h=0.2 m, 1 m, 2 m, 3 m
		150 mm RC wall	h=0.2 m, 1 m, 2 m, 3 m
	250 mm RC slab	150 × 150 mm RC column @5 m	h=3 m
	300 × 300 mm RC beam @5 m	150 × 150 mm RC column @5 m	h=3 m

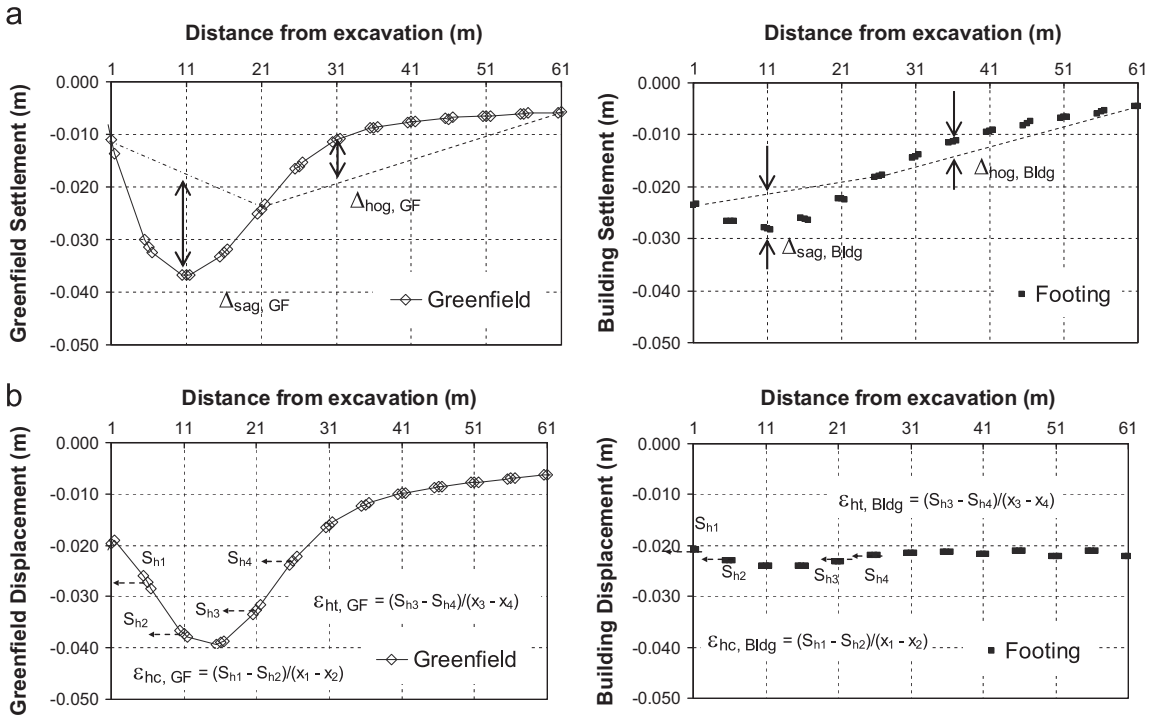

Fig. 18. Surface settlement and horizontal displacement profiles for greenfield and for frame on individual footings (e=1 m). (a) Surface settlement profiles and (b) Horizontal displacement profiles.

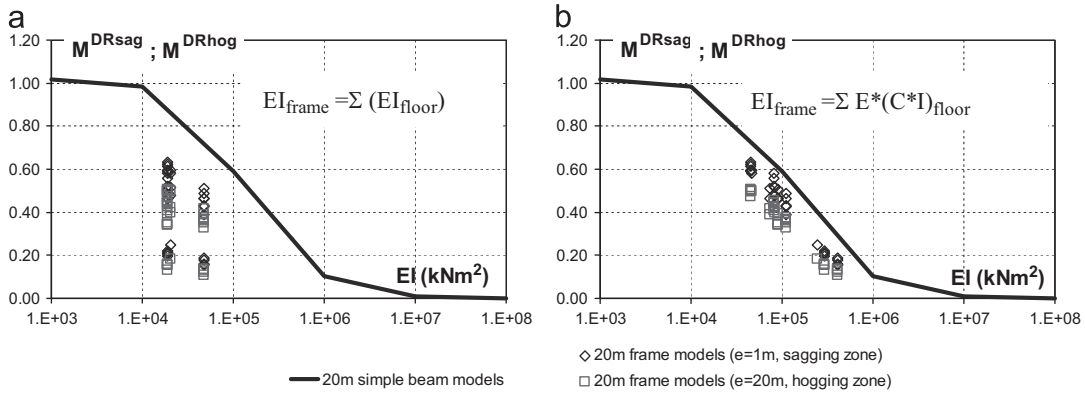

Fig. 19. Deflection ratio modification factors for 20 m long frames on individual footings.

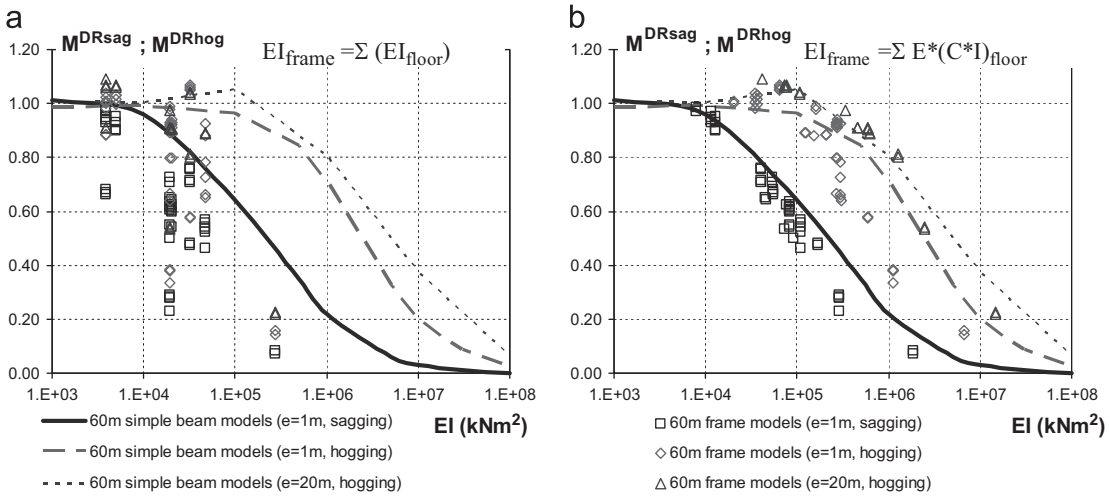

Fig. 20. Deflection ratio modification factors for 60 m long frames on individual footings.

first floor tie-beam (K_B). When the modification factors in Fig. 20 are re-plotted against this frame stiffness factor, the results from the different frame-on-individual-footing models appear to be closely grouped, as seen in Fig. 23.

In a similar way, the horizontal strain modification factors for the 20-m frame models with 1-m and 20-m eccentricity and the 60-m frame models with 20-m eccentricity can be plotted against their frame stiffness factors. Fig. 24 shows the modification factor plots for all the models of frames on individual footings, from which a reasonable upper bound curve drawn for all the points can be used as design guidance. This can be used for considering the influence of frame stiffness to estimate horizontal strains in frame buildings on individual footings, or buildings on strip footings that are transverse to the induced deformation trough.

4.4. Design guidance to estimate horizontal strains

Using a simple portal frame to derive the frame stiffness factor is clearly a simplification of the actual problem. In reality, frame structures would have bays of different lengths as well as different numbers of upper storeys that would have an influence on the framing action at the ground floor. It is also recognised that the portal frame in the structural analysis was pin-supported, whereas the footing foundation in an actual building would restrain the rotation of the ground floor columns, and the extent of this restraint – depending on the footing stiffness – would also have an influence on the frame stiffness. Infill walls within the frame structures are usually not structurally monolithic to the frame structure, and it is reasonable to ignore their contribution to frame stiffness – unless the walls are designed as shear walls and would therefore be additive to building stiffness.

Nevertheless, a reasonable upper bound can be derived from amongst all the frame models whose structural elements were varied. For example, additional finite element models were completed for various frame models, shown in Table 6, where a rough soil–footing interface was modelled to transfer the maximum shear stress between the soil and the footing, and under different excavation configurations, as summarised in Table 7. Although there are significant differences in the magnitude of the maximum horizontal strains for the same building between the various excavation models, the modification factors of horizontal strain when plotted against the frame stiffness factor (Fig. 25) fall within the upper bound curve. This suggests that the ability of a frame building in resisting horizontal strains between the individual footings may be more dependent on the structural stiffness of the frame than on the underlying soil profile or the foundation–soil interface condition.

Finally, design guidance defined using an upper bound curve will estimate higher horizontal strains for framed buildings on individual footings – this is conservative, but acceptable. Nevertheless, it is noted that there is a significant spread in the modification factors corresponding to each frame structure. It may be possible to reduce the spread by defining a more refined frame stiffness factor through a more rigorous structural analysis, which could also make the frame stiffness factor dimensionless, but the refined factor may be more difficult to estimate in practice.

5. Conclusions

The influence of frame action on building response has been investigated in this paper. This was done by constructing finite element models of frame structures with various configurations behind a multi-propped excavation in soft clay, firstly for buildings on continuous footings, and also for buildings on individual footings.

By re-formulating Meyerhof's derivation to quantify the stiffening effect of columns on a beam line in a frame building, a modified column stiffening factor was defined to estimate the bending stiffness of frame structures. The column stiffening factor was different from the original Meyerhof derivation in two ways – firstly, the Young's modulus of the beams and the columns was included to extend its application to composite frames, and secondly, the sagging length and hogging length

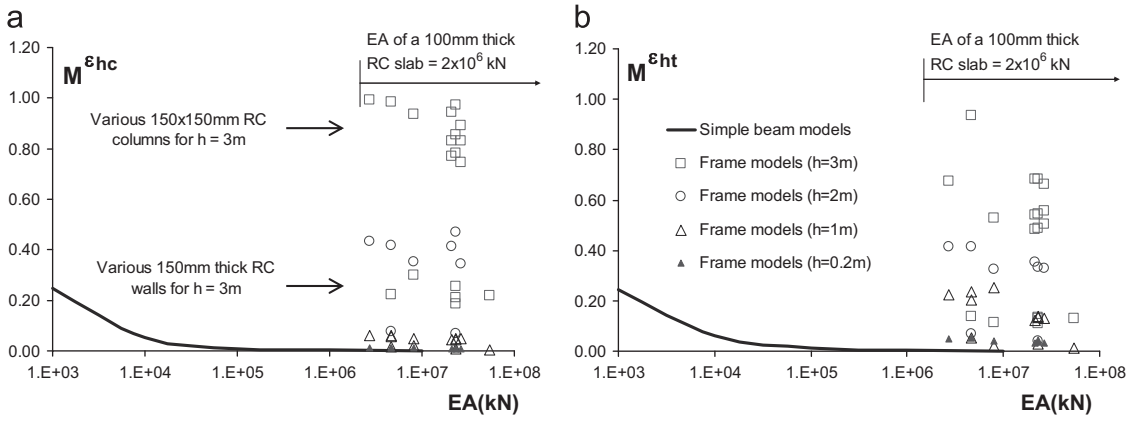

Fig. 21. Horizontal strain modification factors of 60 m long frames on individual footings with various axial stiffness values.

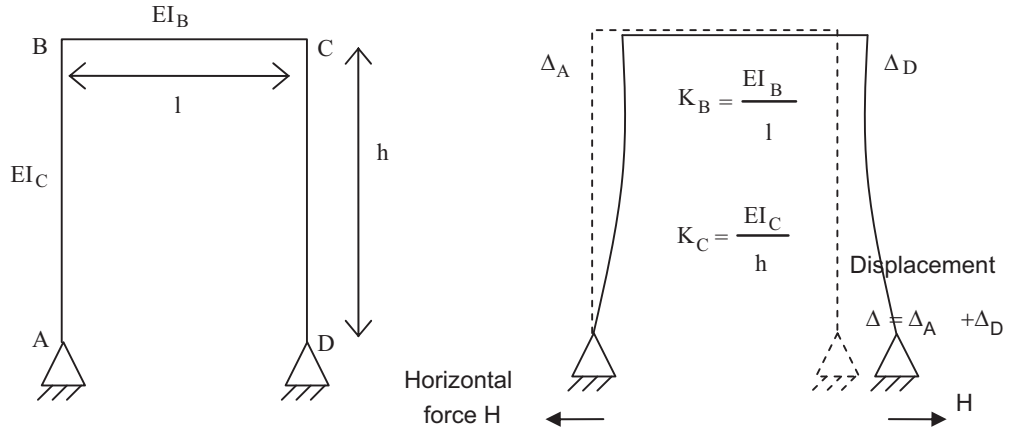

Fig. 22. Schematic of the simple portal frame.

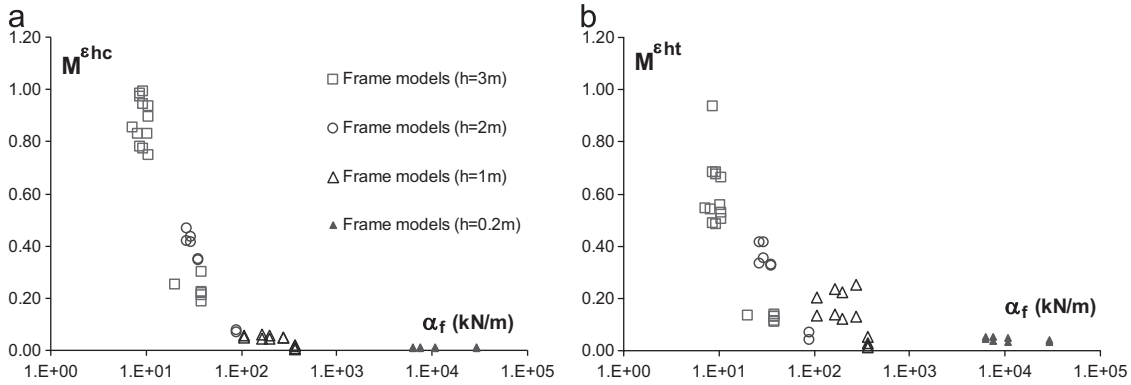

Fig. 23. Horizontal strain modification factors for different frame stiffness factors of 60 m long frames on individual footings.

were used instead of the length of the entire building. By comparing the finite element results of the frame models with simple beam models, the bending behaviour of frame structures was found to be well approximated to a simple beam model when the column stiffening factor was used. After estimating the contribution to building stiffness due to its framing action, designers can then refer to the guidance developed for the building response to tunnelling- and excavation-induced movements using simple beams (such as the charts by Franzius et al., 2006, Goh and Mair 2011b, and Goh and Mair 2011c) and obtain a more realistic estimate of building behaviour. As an alternative, the simpler method of algebraically summing the bending stiffness of each individual floor beam – and ignoring any frame action – is also reasonable, but less accurate. This holds true for both frames on continuous footings and frames on individual footings.

In contrast to settlement behaviour, the horizontal displacement responses are different between frames on continuous footings and frames on individual footings. Whilst horizontal strains are usually negligible for frames on continuous

footings, they are significant for frames on individual footings even when the axial stiffness of the frame building is high. The greatest horizontal strains occur at the ground floor between individual column footings, and were observed to be related to the frame properties at the ground floor. Using a structural analysis of a simple, pin-supported portal frame, a new frame stiffness factor has been defined to describe the horizontal stiffness of a frame structure. By plotting the horizontal strain modification factor against the frame stiffness factor, an upper bound curve has been developed to suggest guidance for estimating the maximum horizontal strains in rigidly connected frame buildings that are on individual footings – including buildings on strip footings that are transverse to the induced ground displacement troughs.

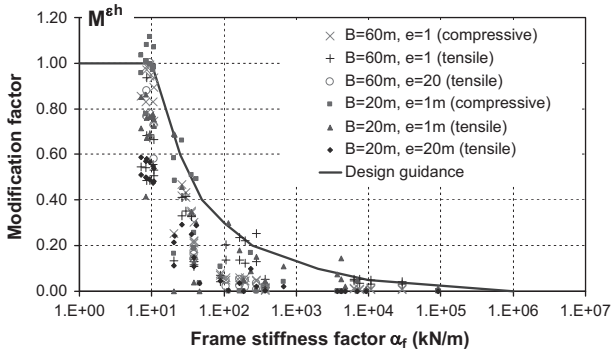

Fig. 24. Horizontal strain modification factors for frames on individual footings with slipping interface.

Furthermore, the influence of infill walls on the stiffness of framed buildings was ignored; this is reasonable for most cases where such infills are not structurally connected to the building frame, unless the walls are designed as shear walls. In the latter, the stiffness of the shear walls could be estimated using an equivalent deep beam, and would add to the building stiffness arising from the frame actions discussed in this paper.

This paper only considers the frame action of buildings on shallow foundations and ignores the influence of any soil–pile interaction. The key influence of pile foundations, due to various construction effects, should be considered separately (e.g., Tamura et al., 2012).

Finally, it has to be noted that this study using frame models relates to the inclusion of building stiffness in estimating deflection ratios and horizontal strains from the greenfield condition. This does not mean that the response of a framed building is the same as a simple beam or that the damage to a framed building can be fully described using a simple beam model. The actual damage to a framed structure, due to ground movements, depends on the re-distribution of loads and strains amongst its frame elements. This is influenced by its member properties and loading patterns, and can only be studied in a detailed structural analysis for each framed building. Nevertheless, Burland and Wroth (1974) conceptualised the limiting tensile strain method using an elastic beam representation as a simple means to identify the damage to buildings, including those with framed structures. The findings presented in this paper should be viewed as an attempt to quantify the influence of building stiffness in the context of the limiting tensile strain method. The influence of frame stiffness is to reduce the

Table 6
Variation of 60 m long, 2-storey frame models with rough soil–footing interface.

Beam type	First floor tie-beam type	Column type	Distance between first floor tie beam and ground footing
100 mm RC slab, with 5 m bay length	100 mm RC slab	150 × 150 mm RC column @5 m	h=1 m, 3 m, 5 m, 10 m
		150 mm RC wall	h=3 m, 5 m, 10 m
	300 × 300 mm RC beam @5 m	150 × 150 mm RC column @5 m	h=1 m, 3 m, 5 m, 10 m
	250 mm RC slab	150 × 150 mm RC column @5 m	h=1 m, 3 m, 5 m, 10 m
		150 mm RC wall	h=3 m, 5 m, 10 m
250 mm RC slab, with 5 m bay length	100 mm RC slab	150 × 150 mm RC column @5 m	h=3 m, 5 m, 10 m
		250 mm RC wall	h=3 m, 5 m, 10 m

Table 7
Variation of soil profiles for 20 m deep excavation.

Model	UD_A	UD_B	UD_H	UD_L
Excavation depth	20 m	20 m	20 m	20 m
Soil profile above stiff bearing layer	20 m thick soft clay	30 m thick soft clay	12 m soft clay+8 m firm soil	12 m soft clay+8 m weathered soil
Wall depth	25 m	35 m	25 m	25 m
D-wall thickness	0.8 m	1 m	0.8 m	0.8 m
No. of props	6 nos.	6 nos.	6 nos.	6 nos.
Pt of inflexion	21 m	29 m	18 m	14 m

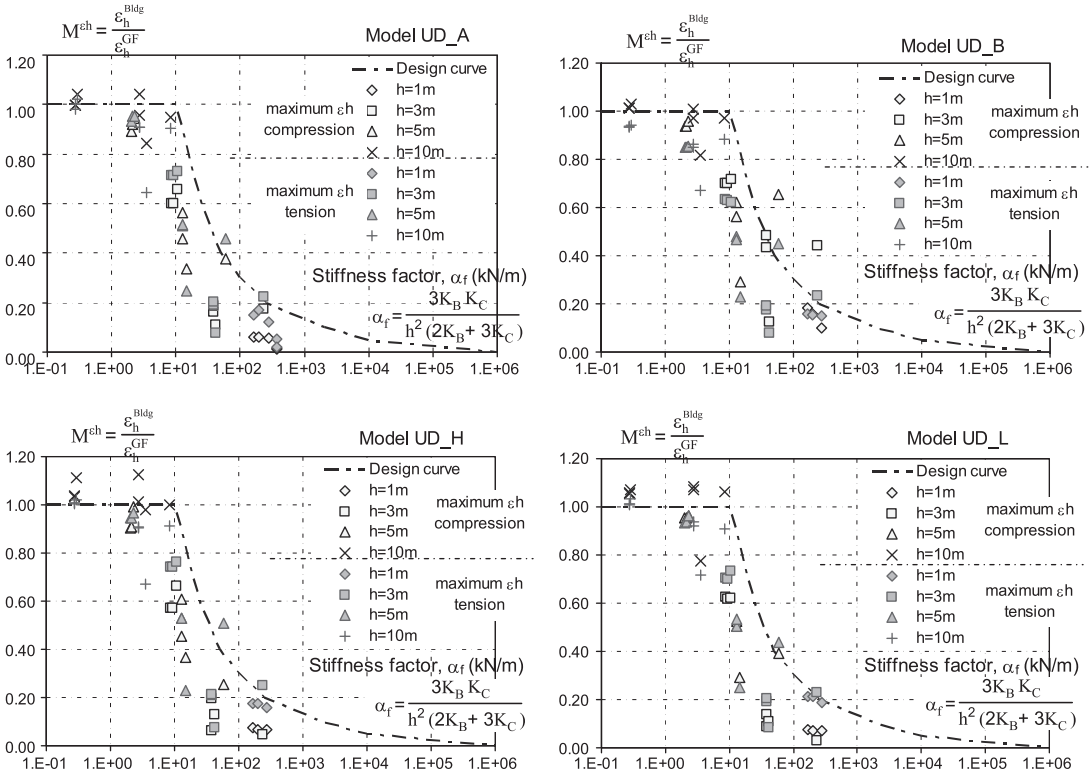

Fig. 25. Horizontal strain modification factors for various frames at 1 m behind excavation with rough interface.

greenfield deflection ratios and horizontal strains using the proposed methods, so that a more realistic tensile strain can be estimated in Stage 2 of the building damage assessment procedure outlined by Mair et al. (1996). The reader should not be misled into thinking that the response of frame buildings can be approximated as simple beam behaviour or vice versa.

References

Burland, J.B., Broms, B.B. and de Mello, V.F.B. 1977. Behaviour of foundations and structures: state-of-the art report. In: Proceedings of the ninth International Conference on Soil Mechanics and Foundation Engineering, Tokyo, 2, pp. 495–546.

Burland, J.B. and Wroth, C.P. 1974. Settlement of buildings and associated damage: Session V review paper. In: Conference on Settlement of Structures, Cambridge, April 1974 , Pentch Press, London, pp. 611–654.

BRE Digest 251, 1995. Assessment of damage in low rise buildings with particular reference to progressive foundation movements, revised. Building Research Establishment, Watford.

Chong, P.T. 2002. Characterisation of Singapore Lower Marine Clay (Ph.D. thesis). National University of Singapore, Singapore.

Dimmock, P.S., Mair, R.J., 2008. Effect of building stiffness on tunnelling-induced ground movement. Tunn. Undergr. Space Technol. 23 (4), 438–450 (2008).

Elshafie, M. Z. E. B. 2008. Effect of Building Stiffness on Excavation Induced Displacements (Ph.D. thesis). University of Cambridge.

Franzius, J.N., Potts, D.M. and Burland, J.B. 2006. The response of surface structures to tunnel construction. In: Proceedings of the Institution of the Civil Engineers, Geotechnical Engineering, 159(1): 3–17.

Goh, K.H. 2010. Response of Ground and Buildings to Deep Excavations and Tunnelling (Ph.D. thesis). University of Cambridge.

Goh, K.H. and Mair, R.J. 2011a. The horizontal response of framed buildings on individual footings to excavation-induced movements. In: Proceedings of the Seventh International Symposium TC28 Geotechnical Aspects of Underground Construction in Soft Ground, May 2011, Rome.

Goh, K.H. and Mair, R.J. 2011b. The response of buildings to movements induced by deep excavations. In: Proceedings of the Seventh International Symposium TC28 Geotechnical Aspects of Underground Construction in Soft Ground, May 2011, Rome.

Goh, K.H., Mair, R.J., 2011c. Building damage assessment for deep excavations in Singapore and the influence of building stiffness. Geotech. Eng. J. SEAGS AGSSEA 42 (3), 1–12 (September 2011).

Lambe, T.W., 1973. Prediction in soil engineering. Géotechnique 23 (2), 149–202.

Leong, E.C., Rahardjo, H., Tang, S.K., 2003. Characterisation and engineering properties of Singapore residual soils. Characterisation and Engineering Properties of Natural Soils, 1. Swets & Zeitlinger, Lisse, 1279–1304.

Liew, Y.K., Veluvolu, H., Kho, C.M. and Sigl, O. 2008. Risk assessment for earth pressure balancing bored tunnelling under shophouses along Pasir Panjang Road. In: Proceedings of the International Conference on Deep Excavations, 10–12 November 2008, Singapore.

Mair, R.J., Taylor, R.N., Bracegirdle, A., 1993. Sub-surface settlement profiles above tunnels in clays. Geotechnique 43 (2), 315–320.

Mair, R.J. 2003. Keynote lecture: Research on tunnelling-induced ground movements and their effects on buildings – lessons from the Jubilee Line Extension. In Jardine, F.M. (Ed.), Response of Buildings to Excavation Induced Ground Movements, Proceedings of International Conference, London, 17–18 July 2001: 3–26. London: CIRIA.

Mair, R.J. and Taylor, R.N. 1997. Bored tunnelling in the urban environment: state-of-the-art report and theme lecture. In: Proceedings of the Fourteenth International Conference on Soil Mechanics and Foundation Engineering, Hamburg, 6–12 September 1997, 4: 2353–2385. Balkema, Rotterdam.

Mair, R.J., Taylor, R.N., 2001a. Elizabeth house: settlement predictions. In: Burland, J.B., Standing, J.R., Jardine, F.M. (Eds.), Building Response to tunnelling – Case studies from construction of the Jubilee Line Extension, London, Vol. 1. Thomas Telford, London, pp. 195–215 (Projects and Methods).

Mair, R.J., Taylor, R.N., 2001b. Settlement predictions for Neptune, Murdoch, and Clegg Houses and adjacent masonry walls. In: Burland, J.B., Standing, J.R., Jardine, F.M. (Eds.), Building Response to tunnelling – Case studies

from construction of the Jubilee Line Extension, London, Vol. 1. Thomas Telford, London, pp. 217–228 (Projects and Methods).

Mair, R.J., Taylor, R.N. and Burland, J.B. 1996. Prediction of ground movements and assessment of risk of building damage due to bored tunnelling, In: Mair, R.J., Taylor, R.N. (Eds.), Proceedings of the International Symposium on Geotechnical Aspects of Underground Construction in Soft Ground, London, 15–17 April 1996: 713–718. Rotterdam: Balkema.

Meyerhof, G.G., 1953. Some recent foundation research and its application to design. The Structural Engineer 31, 151–167.

Potts, D.M. and Addenbrooke, T.I. 1997. A structures influence on tunnelling-induced ground movements. In: Proceedings of the Institution of the Civil Engineers, Geotech. Engineering 125(2): 109–125.

Tan, T.S., Phoon, K.K., Lee, F.H., Tanaka, H., Locat, J., Chong, P.T., 2003. A characterisation study of Singapore Lower Marine Clay. Characterisation and Engineering Properties of Natural Soils, 1. Swets & Zeitlinger, Lisse 429–454.

Tamura, S., Adachi, K., Sakamoto, T., Hida, T., Hayashi, Y., 2012. Effects of existing piles on lateral resistance of new piles. Soils Found. 52 (3), 381–392.

Tanaka, H., Locat, J., Shibuya, S., Tan, T.S., Shiwakoti, D.R., 2001. Characterization of Singapore, Bangkok, and Ariake clays. Can. Geotech. J. 38 (2), 378–400.

Venkta, R., Hoblyn, S., Mahatma, S. and Lim, H.C. 2008. EPB tunnelling under 2-storey shophouses in mixed face conditions. In: Proceedings of the International Conference on Deep Excavations, 10–12 November 2008, Singapore.